IPI Letters
ISSN 2976 - 730X
IPI Letters 2025,Vol 3 (3):18-33
https://doi.org/10.59973/ipil.242
Received: 2025-07-03
Accepted: 2025-07-11
Published: 2025-07-14

Article

Four Cubes: On the Necessity of Four-Dimensional Perception

Szymon Łukaszyk[1,*]

[1]Łukaszyk Patent Attorneys, Głowackiego 8, 40-052 Katowice, Poland

[*]Corresponding author: szymon@patent.pl

Abstract The study aimed to demonstrate that the perceived (3+0i)-dimensional space is necessary for biological evolution due to the exotic $\mathbb{R}^4$ property of such a space, which ensures variations of traits between individuals perceiving the same differentiable structures. Properties of graphs constructed in Boolean spaces $\{0,1\}^n$ were researched. The cotan Laplacian of 2-face triangulated n-cube was shown to have a spectrum corresponding to the Hamming distance distribution of Boolean space, and its regular version was shown to be a Ramanujan graph for $2 \leq n \leq 5$ with the smallest integral Ramanujan bound for $n = 4$. The spectrum of the distance matrix on the graph comprising 2^n n-cubes sharing a common origin was shown to be bounded by irrational eigenvalues, and if its 2-faces are triangulated, the spectrum of the cotan Laplacian includes all integers from 0 to $3n$ without the eigenvalue of $3n-1$. The relations of these graphs with Buckminster Fuller's vector equilibrium were discussed. Based on Watanabe's ugly duckling theorem, we defined a trainable activation function of an artificial neuron in a sparse distributed memory model.

Keywords Boolean spaces; Spectral graph theory; Sparse distributed memory; Activation functions; Neural architectures; Geometric deep learning; Cotan Laplacian; Exotic $\mathbb{R}^4$; Vector equilibrium; Ramanujan graphs; Topological data analysis; Emergent dimensionality

1 Introduction

All we perceive is information measured in bits, which are the quanta of information. On the other hand, we perceive nature now in one, unidirectional temporal dimension and three, bidirectional spatial dimensions. We can therefore assume that spatial dimensions are real, while the temporal dimension is imaginary [1]. However, the natural question is, why do we perceive nature in such a dimensionality? It does not result from the free energy principle [2], which offers a formal description of self-organizing structures [3], including us, the living systems. Perhaps there are individuals (*flatlanders*?) perceiving their universe(s) in n dimensions, with $n \neq 3$ spatial ones? Pseudo-Riemannian manifolds used in general relativity theory are not bound to four dimensions. The combinatorial proof of Boltzmann's H-theorem [4] introducing the concept of energy quantization, which led to the development of quantum theory [5], is irrelevant to any particular dimensionality of space, in which Ludwig Boltzmann considered the molecules to collide.

The goal of this study was to answer this question and link the perceived spatial-temporal dimensionality with spatial-temporal independent [6-8] information through the perception of a biological entity and in an information-theoretic approach. Although this goal has not been completed, this study presents some non-physical patterns [9] we found while pursuing it.

The paper is structured as follows. Section 2 presents certain properties of three graphs constructed in Boolean spaces: n-cube 2.1, $\{n\}$-cube 2.2, and $[n]$-cube 2.3 and hints at their applications. If 2^n of such graphs are oriented in space to share a common vertex, they form a larger graph similar to Buckminster Fuller *Vector Equilibrium*, which is discussed in Section 3. Section 4 discusses the goal and findings of this study in the context of $n = 4$.

2 The Cubes

We begin by outlining three cubic graphs that can be constructed in $\{0, 1\}^n$ Stone space (Boolean space), $n \in \mathbb{N}$, on the set of 2^n vertices, where a distinct index $m = 1, 2, \cdots, 2^n$ and a distinct address $a(m)_n = \{b_1, b_2, \cdots, b_n\}$, $b = \{0, 1\}$ are assigned to each vertex (hereinafter by "a vertex m" we mean "a vertex index m"). If we define

$$a(1)_1 \coloneqq 0, \quad a(2)_1 \coloneqq 1, \quad m_1 \coloneqq 1, 2, \ldots, 2^{n-1}, \quad m_2 \coloneqq 2^{n-1} + 1, 2^{n-1} + 2, \ldots, 2^n, \tag{1}$$

then a Gray code address $a(m)_n$ can be assigned to a vertex m recursively as

$$a(m)_n \coloneqq \begin{cases} \{0, a(m)_{n-1}\}, & m \in m_1, \\ \{1, a(2^n - m + 1)_{n-1}\}, & m \in m_2, \end{cases} \tag{2}$$

so that the subsequent addresses $\{a(m)_n, a(m \pm 1)_n\}$ differ by just one bit. Similarly a binary code address $a(m)_n$ can be assigned to a vertex m recursively (left-msb) as

$$a(m)_n \coloneqq \begin{cases} \{0, a(m)_{n-1}\}, & m \in m_1, \\ \{1, a(m - 2^{n-1})_{n-1}\}, & m \in m_2, \end{cases} \tag{3}$$

where $\operatorname{dec}(a(m)_n) = m - 1$. Binary addresses $a(m)_n$ can also be randomly assigned to a vertex set. Each pair of addresses $a(k)$ and $a(l)$, $k, l \in \mathbb{N}$ define a Hamming distance $d_{\mathrm{HM}}(a(k), a(l))$ between them that can be arranged in a $2^n \times 2^n$ distance matrix

$$D_{k,l} \coloneqq d_{\mathrm{HM}}(a(k), a(l)). \tag{4}$$

The 1st graph, n-cube, has edges between addresses providing unit Hamming distances; the 2nd one, $\{n\}$-cube, has edges between all vertices; and the 3rd one, $[n]$-cube, has triangulated 2-faces. The first two graphs are commonly known.

2.1 n-cube

n-simplicial complexes of discrete exterior calculus disentangle the topological (metric-independent) and geometrical (metric-dependent) content of the modeled quantities [10], keeping their intrinsic structure intact. Operators, which in the continuous theory do not use metric information, maintain this property in the discrete theory as well [11]. Thus, at least in this regard, the simplex formulation is equivalent to continuous calculus, allowing for an easier discovery of local and global invariants which are often difficult to recognize if written in tensorial notation [10].

n-cube, having $\binom{n}{k} 2^{n-k}$ k-faces is the smallest proper n-dimensional hole that can be created in a simplicial n-manifold. Removing just one n-simplex could not serve as a model of a hole, as one removes only this internal n-simplex *volume*, leaving all its facets intact. Thus, Stokes integration over an n-manifold with one missing n-simplex, not on the boundary of that manifold, is the same as if this n-simplex were present. Also, an n-orthoplex (dual to n-cube) could not be a proper hole, since the general formula $2^{k+1}\binom{n}{k+1}$ for the number of k-faces of n-orthoplex vanishes[1] for $k = n$, so that it formally does not have an n-face Besides, all the remaining 2^n facets of n-orthoplex (just like all the $n + 1$ facets of n-simplex) are $(n - 1)$-simplices, while all the $2n$ facets of n-cube are also $(n - 1)$-cubes. n-orthoplex cannot be prism-like extruded from a point like an n-cube; it is built by adding two vertices along a new orthogonal axis and taking the convex hull, forming simplicial facets. n-cube, n-orthoplex, and n-simplex are the only regular polytopes present in any complex dimension [12].

[1] $\binom{n}{n+1} = 0$ if the binomial coefficient is defined in terms of a falling factorial.

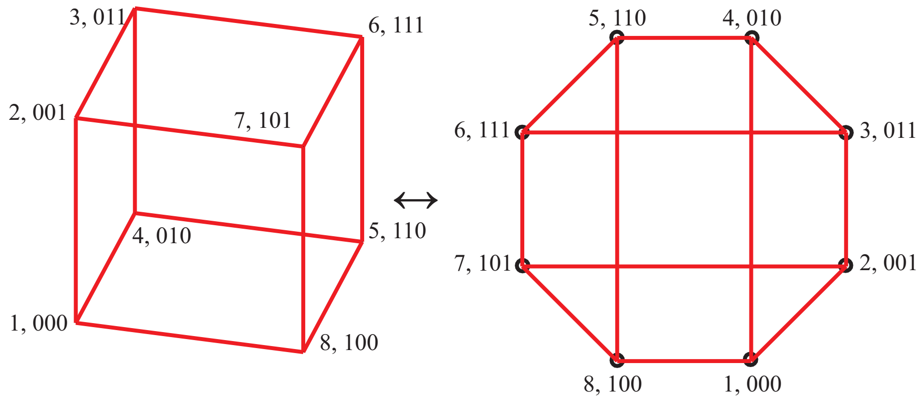

Figure 1: Gray encoded 3-cube with its associated bipartite graph.

The orthogonal edges of n-cube originating from the vertex having the address $a(m) = \{0, \ldots, 0\}$ in a way define a 2^{-n} part of a Cartesian coordinate system of Euclidean $\mathbb{R}^n$ space (cf. Fig. 6). Furthermore, as shown in Fig. 1, if the addresses $a(m)$ of the vertices of n-cube are ordered using Gray code (2), n-cube is a bipartite graph with the first set containing even vertex indices and the second set containing odd indices.

2.2 $\{n\}$-cube

$\{n\}$-cube, shown in Fig. 2 for $n \in \{2, 3\}$, represents Boolean space and it is easily seen that it is isomorphic to $(2^n - 1)$-simplex and hence has a $\binom{2^n}{k+1}$ of k-faces. On the other hand, a regular n-simplex can be inscribed in an n-cube (using only a subset of the set of its vertices) if and only if $n = 2^m - 1$ for $m \in \mathbb{N}_0$ [13]. The degree of a vertex of $\{n\}$-cube is $2^{1-n}\binom{2^n}{2}$ which is an odd number.

Based on the properties of this complete graph, Pentti Kanerva [14] introduced the concept of sparse distributed memory (SDM), a mathematical model for the memory and learning processes of animals provided with neural networks. Sparseness reflects his hypothesis that not all addresses $a(m)$ of the address space are implemented. The main attribute of this model is sensitivity to similarity, meaning that information can be read back not only by giving the original write address but also by giving one close to it, as measured by the number of mismatched bits (i.e., the Hamming distance between memory addresses). The SDM model features *knowing that one knows* and *tip of the tongue* phenomena present in biological autonomous learning systems, such as the human brain, that base their operation on an internal model of the world, which they build through experience [14]. The SDM is particularly notable for its ability to store and retrieve high-dimensional binary patterns in a robust, distributed manner [14]. Various architectures of artificial neural networks utilizing the properties of $\{n\}$-cube have been proposed and used for various applications, including vision-detecting, robotics, signal detection, etc.

The number of addresses that are exactly k bits from an arbitrary address $a(m)$ is the number of ways to choose k coordinates from a total of n coordinates. Thus, it is given by the binomial coefficient $\binom{n}{k}$. An outstanding property of $\{n\}$-cube is that the mean Hamming distance between any address a_m and all the other addresses (including a_m) is $n/2$ (variation is $n/4$). If an $\{n\}$-cube were inscribed in the closed n-ball with two of its vertices defining the poles, then most of the remaining vertices would lie at or near the equator. This is called a *tendency to orthogonality* [14].

Properties of $\{n\}$-cube have also been studied by Satosi Watanabe in a framework of *Epistemological Relativity* [15]. He noted that each k^{th} bit of an address $a(m)$ could be considered a certain Boolean-valued starting predicate Q_k that can be meaningfully applied to some set of objects. He termed an address $a(m)$ a disjoint atomic predicate that can be expressed as a conjunction of starting predicates

$$a(m) = \bigcap_{k=1}^{n} a_{mk} Q_k, \tag{5}$$

where $a_{mk} = 1$ if $a(m)$ contains Q_k under the conjunction, and $a_{mk} = 0$ if a_m contains the negation of Q_k under the conjunction. In this approach, starting predicates Q_k are unrelated to the *spatial* addresses of

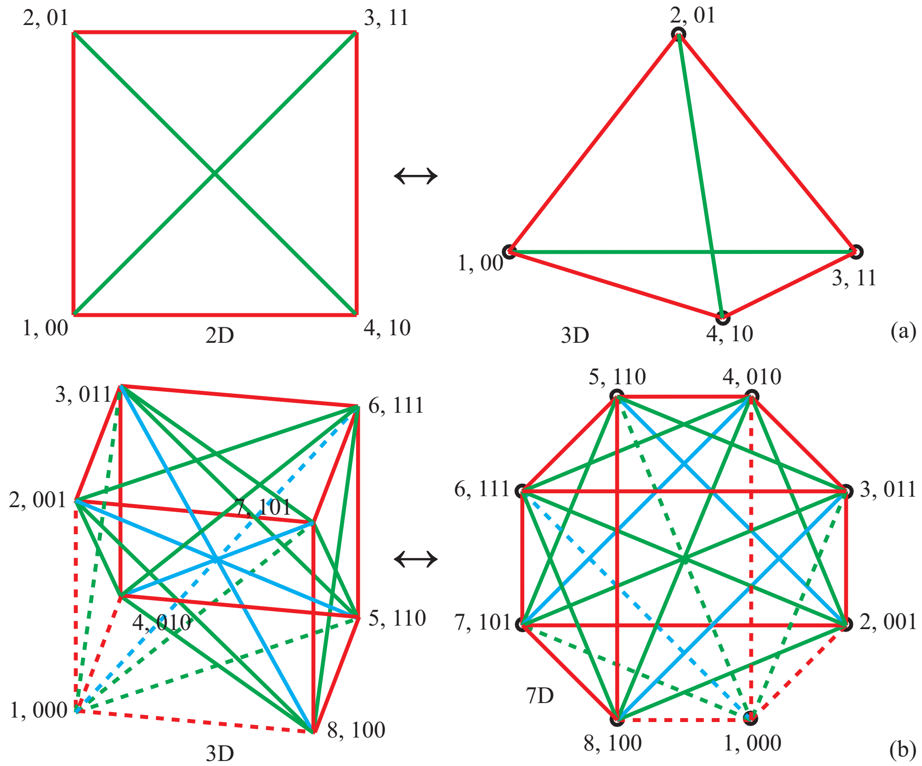

Figure 2: (a) {2}-cube and 3-simplex; (b) {3}-cube and 7-simplex. Gray encoding. RGB colors denote increasing Hamming distances between addresses of the vertices. Dashed lines symbolize rank 2 compound predicates A_s (edges) related to a vertex $m = 1$, and the number of distinct colours is related to the number of degenerate eigenvalues of the cotan Laplacian of [3]-cube.

the vertices. Address $a(7) = \{101\}$ in Gray encoding, for example, can be formed from true predicates $Q_1 = 1$, $Q_2 = 1$, and $Q_3 = 1$ using coefficients $a_{71} = 1$, $a_{72} = 0$, and $a_{73} = 1$.

Watanabe also considered Boolean-valued compound predicates A_s ($s = 1, 2, \ldots, 2^{2^n}$), all the logical functions that can be formed from the starting predicates Q_k, with connectives of negation, conjunction, and disjunction. For $\{n\}$-cube, they can also be expressed as a disjunction of vertices

$$A_s = \bigcup_{m=1}^{2^n} A_{sm}, \tag{6}$$

where $A_{sm} = 1$ if A_s contains a vertex m under the disjunction and 0 otherwise, so $A_s = \{00\ldots0\}$ denotes the empty set ($\emptyset$) containing no vertices and $A_s = \{11\ldots1\}$ denotes the Power set ($\square$) containing all 2^n vertices. The sum of ones in the compound predicate A_s is the rank r of this predicate or the number of vertices it is built upon. Compound predicates form a half-ordered Boolean lattice in the sense that there are implicational relations $A_s \Rightarrow A_t$ between predicates A_s, A_t, providing that $\text{rank}(A_s) < \text{rank}(A_t)$. An implicational relation $A_s \Rightarrow A_t$ is equivalent to $A_{sm} \leq A_{tm}, \forall m$, in other words $A_{sm} = 1 \Rightarrow A_{tm} = 1\ \forall m$. Furthermore, any compound predicate A_s satisfies $\emptyset \Rightarrow A_s \Rightarrow \square$. Compound predicates A_s can be thought of as k-simplices of a $(2^n - 1)$-simplex isomorphic to $\{n\}$-cube with:
(-1)-simplex as the empty set $\emptyset$ (rank 0 predicate A_s);
0-simplices as vertices (rank 1 or atomic predicates A_s);
1-simplices as edges (rank 2 predicates A_s);
2- simplices as triangles (rank 3 predicates A_s);
3- simplices as tets (rank 4 predicates A_s);
$\ldots$;
k- simplices (rank $k + 1$ predicates A_s);
and so on up to the single $(2^n - 1)$-simplex spanned on all the vertices of the $\{n\}$-cube.

Watanabe [15] assumed that an object satisfies or negates each starting predicate Q_k. In other words, any object corresponds to a vertex of $\{n\}$-cube. This assumption is the identity of indiscernibles ontological principle, stating that separate *objects* cannot have all their properties in common (this *principle* is false in the quantum domain [16]. With this assumption in place, a compound predicate A_s of rank $r \geq 2$ (at least an edge) would be shared by p objects if it included p vertices corresponding to these objects. The number of predicates A_s of rank $r \geq 2$ shared by p objects (vertices)

$$N_{r,p} = \binom{2^n - p}{r - p} \tag{7}$$

is the same for any p objects to which these predicates A_s are applicable (two objects share 1 edge, three objects share 1 face of $(2^n - 1)$-simplex, etc.). Watanabe regarded the number of shared predicates as a measure of similarity and the number of not shared predicates as an indication of dissimilarity [17]. Therefore, any two objects, insofar as they are distinguishable (i.e., correspond to different vertices), are equally similar. This is Watanabe's famous ugly duckling theorem (UDT). As a *corollary* (or rather a relief) to the UDT, Watanabe suggested [15] that one has to ponderate (give weights to) the predicates A_s to assert the similarity of the objects: for two objects to be more similar to each other, they have to share some more important (more weighty) predicates.

In the SDM, $\{n\}$-cube models a single neuron, where the vertices play the role of synapses, the points of electric contact between neurons, or simply the neuron inputs. The activation function of an artificial neuron defines the output of that neuron given the set of inputs. Only nonlinear activation functions allow neural networks to compute nontrivial problems. Their important characteristic is that they provide a smooth, differentiable transition as input values change, i.e., a small change in input produces a small change in output. A neuron *fires* when the activation function exceeds a specific activation threshold. One of the most popular [18] nonlinear activation functions is the logistic (aka sigmoid) one

$$f_l(r) = \frac{1}{e^{-\mu r} + 1}, \tag{8}$$

where $r \in \mathbb{R}$ is the weighted sum of the neuron inputs and μ is a parameter (here we take $\mu = 1$)[2]. Softplus

$$f_{\text{sp}}(r) = \ln(e^r + 1) \tag{9}$$

is another example of such a function.

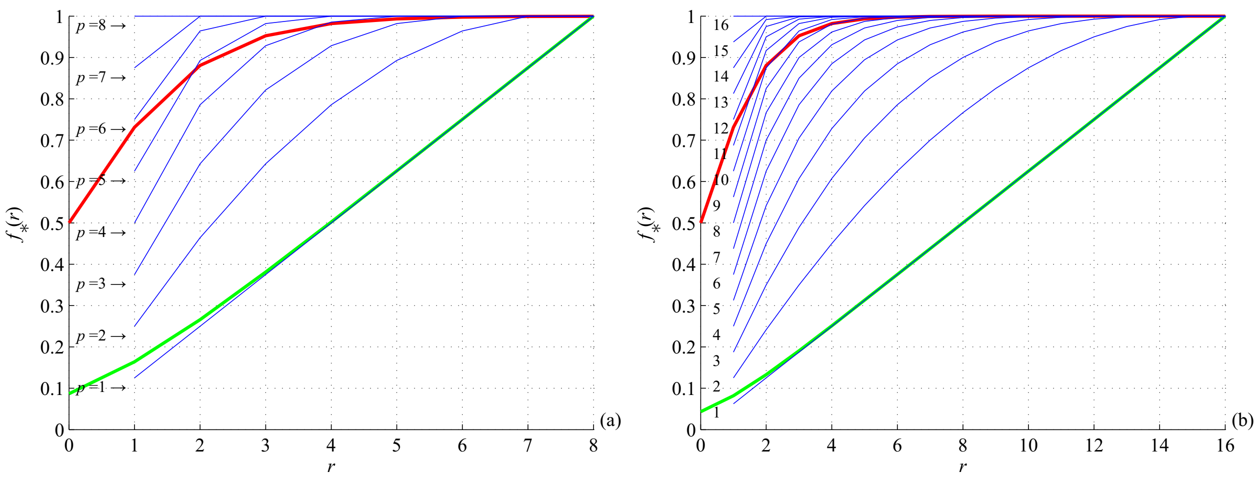

Figure 3: Logistic $f_l(r)$ (red), softplus $f_{\text{sp}}(r)/2^n$ (green), and $\{n\}$-cube $f_{\{n\}}(r)$ (blue) activation functions. (a) {3}-cube, (b) {4}-cube.

If we now assume that the vertices of $\{n\}$-cube are synapses, then it remains to define the activation function and assume a certain activation threshold. We note that

$$N_{r,1} = \binom{2^n - 1}{r - 1} \quad \text{out of} \quad \binom{2^n}{r} \tag{10}$$

rank r available compound predicates A_s (6) of rank $r \geq 1$ are related to one vertex. For {3}-cube, for example, one vertex is related to 1 (out of 8) rank 1, 7 (out of 28) rank 2, 21 (out of 56) rank 3, 35 (out of

[2]In particular, in parts of the range $\mu \in [0, 4] \vee [-2, 4]$, the logistic map $x_{n+1} = \mu x_n(1 - x_n)$, which is analogous to the logistic function derivative $f'(x) = \mu f(x)(1 - f(x))$ displays intermittent (irregular alternation of periodic and chaotic dynamics) behavior.

70) rank 4, 35 (out of 56) rank 5, 21 (out of 28) rank 6, 7 (out of 8) rank 7 predicates, and with the whole set of vertices (cf. Fig. 2(b)). The linear sequence $\{1/8, 7/28, 21/56, 35/70, 35/56, 21/28, 7/8, 1\}$ can be used to define rectified linear activation function of {3}-cube neuron associated with this vertex. In general

$$N_{r,p} = \sum_{l=1}^{p} \binom{2^n - l}{r-1} \quad \text{out of} \quad \binom{2^n}{r} \tag{11}$$

rank $1 \le r \le 2^n$ predicates A_s are related to p vertices, as illustrated in Fig. 3 showing sequences

$$f_{\{n\}}(r, p) = \sum_{l=1}^{p} \binom{2^n - l}{r-1} / \binom{2^n}{r} \tag{12}$$

for {3}-cube and {4}-cube and the logistic (8) and softplus (9) activation functions. In particular $f_{\{n\}}(r, 1) = r/2^n$ and

$$f_{\{n\}}(r, 2) = r\frac{2^{n+1} - 1 - r}{2^n(2^n - 1)}. \tag{13}$$

We see that the relation (12) is undefined both for $r = 0$ and for $p = 0$. For $r \neq 0$, it is linear for $p = 1$, nonlinear for $1 < p < 2^n$, and at $p = 2^n$ it becomes a unit constant function. Thus, we can think of $\{n\}$-cube vertices as elements of a set $\mathcal{P}$ of p *memorized objects* and of another distinct set $\mathcal{R}$ of r *activated synapses* overlapping $\mathcal{P}$, where we demand $\exists m \in \mathcal{P} \cap \mathcal{R}$. Then, the relation (12) can be considered the neuron's vertex-dependent activation function parametrized by p, which makes it trainable [19]. We see that the probability of an $\{n\}$-cube neuron firing increases, as expected, both with the increasing number of r activated vertices, as well as with the increasing number of p memorized vertices, where for $p = 2^n$ the neuron is saturated. Notably, the information capacity of a {3}-cube (8 vertices) could be employed by nature; a neuron has 5-7 dendrites on average [20].

A neuron, as a living biological cell, is a dissipative structure [21], a self-organizing system maintaining a separable joint state [22] with its environment (*Umwelt*) through a 2-dimensional and triangulated [23] holographic screen [24] through which it processes quantum information [25]. That hints at another cube.

2.3 $[n]$-cube

A 2-dimensional triangulated surface allows defining the discrete cotan-Laplace operator, assuming that every relation (edge) between vertex indices k and l carries a real-valued weight

$$\omega_{kl} = \frac{1}{2}\left(\cot \alpha_{kl} + \cot \beta_{kl}\right), \tag{14}$$

where α_{kl} and β_{kl} are the angles opposite the edge between vertices k and l in the two triangles sharing that edge. This equality, called the cotangent formula, has been derived in many different ways and rediscovered many times over the years [26].

If the vertices are ordered, this ordering can be used to induce the orientation of the edges and angles α_{kl} and β_{kl}, as $k < l \Leftrightarrow k \to l$. Then if α_{kl} and β_{kl} are directed towards vertex l, weights ω_{kl} (14) are positive, while if they are directed towards vertex k, weights ω_{kl} are negative

$$\omega_{kl} = \frac{1}{2}\left(\cot(-\alpha_{kl}) + \cot(-\beta_{kl})\right) = -\frac{1}{2}\left(\cot(\alpha_{kl}) + \cot(\beta_{kl})\right). \tag{15}$$

For a *locally disk-like* triangulated manifold allowing at most two triangles incident to an edge, the discrete cotan-Laplace operator acting on a function $u : V \to \mathbb{R}$, where V is a vertex set of this graph, can be defined [27] as:

$$(Lu)_k = \sum_{l \sim k} \omega_{kl}\left(u_k - u_l\right), \tag{16}$$

where the sum ranges over all vertices l that are connected to the vertex k. This allows for representing the linear operator L as a matrix with the entries

$$L_{kl} = \begin{cases} -\omega_{kl} & \text{if } k \neq l \text{ and they are connected} \\ \sum_{m \sim k} \omega_{km} & \text{if } k = l \\ 0 & \text{otherwise} \end{cases}, \tag{17}$$

which is called the weakly defined discrete Laplace matrix or just cotan Laplacian [27]. This is, in general, not the same as Kirchhoff matrix $(G - E)$, where G is the (diagonal) degree matrix and E, the adjacency matrix of the graph. Zeroing ω_{kl} for disconnected vertices encapsulates the locality of action of the Laplacian operator (16): changing the value of u_l at a vertex l does not alter the value $(Lu)_k$ at vertex k if these vertices are unrelated.

We note in passing that in a weighted adjacency matrix, entries pertaining to unrelated vertices should be set to infinity or a suitable large value, as zero in these locations would be incorrectly interpreted as an edge with no distance, cost, etc. Both (14) and (15) guarantee setting such entries to infinity if $\alpha_{kl}, \beta_{kl} \in \{0, \pi\}$. One could say that in this case, such a relation is a *flat relation*.

One may define the gradient ∇u_{kl} between the connected vertices k and l as the finite difference $(u_k - u_l)$. Accordingly, one defines the discrete Dirichlet energy of u as

$$E_D[u] := \frac{1}{2} \sum_{(k,l) \in E} \omega_{kl} (u_k - u_l)^2 = \frac{1}{2} u^T L u, \tag{18}$$

where the sum ranges over all edges between the vertices. Solving the discrete cotan-Laplace equation $Lu = 0$ for all vertices and subject to appropriate boundary conditions is equivalent to solving the variational problem of finding a function u that satisfies the boundary conditions and has minimal Dirichlet energy (18). The Delaunay triangle mesh (dual to the Voronoi one) features many optimality properties: the triangles are the *fattest* possible [28], it maximizes the minimal angles in the triangulation, and more importantly, the Delaunay triangulation of the set of vertices of n-manifold minimizes the Dirichlet energy of any piecewise linear function u over this point set (Rippa's theorem [29]).

In particular, the cotan Laplacian (17):

- is singular (non-invertible), as it has a zero eigenvalue;
- is symmetric (self-adjoint) ($\omega_{kl} = \omega_{lk}$) and thus has real eigenvalues and orthogonal eigenvectors;
- with positive weights (14) it is always positive semi-definite, and with negative weights (15) it is always negative semi-definite (these are not necessary conditions, however [27];
- it has only constant functions u in its kernel [27].

Furthermore, the spectrum of the cotan Laplacian obtains its minimum on a Delaunay triangulation in the sense that the k^{th} eigenvalue of the cotan Laplacian of any triangulation of a fixed point set is bounded below by the k^{th} eigenvalue resulting from the cotan Laplacian associated with the Delaunay triangulation of this point set [28].

The empty circle property of Delaunay triangulation implies that an interior edge is a Delaunay edge iff $\alpha_{kl} + \beta_{kl} \leq \pi$, which is equivalent to $sin(\alpha_{kl} + \beta_{kl}) \geq 0$ or $\cot(\alpha_{kl}) + \cot(\beta_{kl}) \geq 0$. It has been shown [30] that any convex quadrilateral formed by two adjacent triangles, which does not satisfy the empty circle property, may be made Delaunay by *flipping* the diagonal edge of the quadrilateral, common to the two triangles, to the opposite diagonal. This is called a Delaunay flip, and a sequence of Delaunay flips will always converge to a Delaunay triangulation [28]. The borderline case for a Delaunay flip is obviously a rectangle, or a square in particular, having both Delaunay diagonal edges. This leads to the following definition and theorem.

Definition 1. $[n]$-cube is n-cube with triangulated 2-faces.

Theorem 1. Any triangulation of $[n]$-cube generates the same cotan Laplacian.

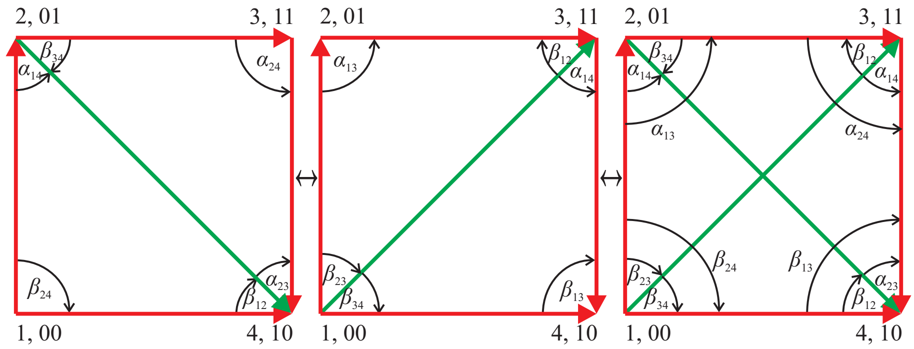

Figure 4: Two diamond graphs on 2-faces of n-cube (here: Gray encoding with positive weights (14)) have the same cotan Laplacian that defines $[n]$-cube cotan Laplacian.

Proof. For 2-face edges $\omega_{kl} = 1$ since $\cot(\pi/4) = 1$ for each angle and for 2-faces diagonals $\omega_{kl} = 0$ since both angles opposite to a diagonal are right angles ($\cot(\pi/2) = 0$). Therefore the coefficients L_{kl} of the matrix (17) are zero not only for disconnected pairs of vertices k and l but also for all pairs of vertices, except for 2-face edges, where $L_{kl} = -1$ and diagonal coefficients where $L_{kk} = n$, as any vertex of n-cube is connected with n 2-face edges (in case of the weights (15) signs of L_{kl} are reversed). □

Technically, cotan Laplacian for $[n]$-cube, shown in Figs. 4, 5, can be easily produced from the distance matrix D (4) by setting $L_{kk} = n$, negating ones and zeroing all the other entries (in case of the weights (15), the signs are reversed). Since $\cot(\pi/2) = 0$, only the ordering of the vertex indices (Gray, binary, etc.) changes the form of the cotan Laplacian.

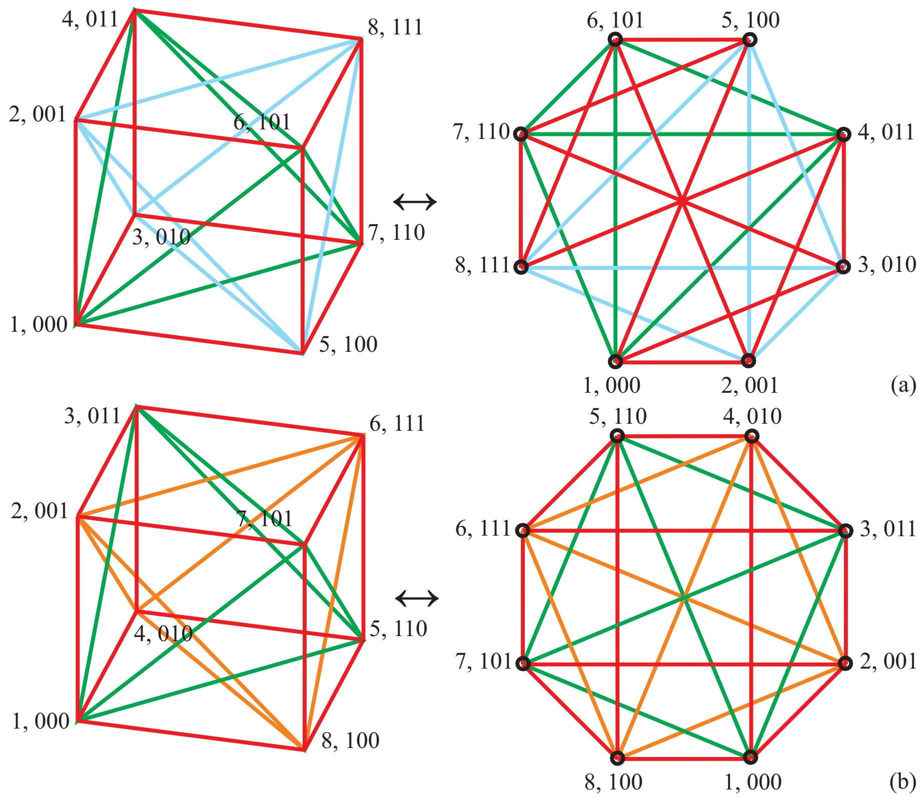

Figure 5: [3]-cube. (a) binary, encoded (b) Gray encoded. For Gray encoding, colors represent even (orange) and odd (green) arrangements of 2-face diagonals.

Theorem 2. For $n > 2$, the eigenvalues of the cotan-Laplacian of $[n]$-cube correspond to twice the binomial distribution of Hamming distances between any address $a(m)$ and addresses of all vertices. For the weights (14) 0 is the minimum eigenvalue; for the weights (15) 0 is the maximum eigenvalue, and the distances are negative.

Proof. Direct calculation for consecutive n. □

Theorem 2 is interesting since the defining equation (17) is unrelated to the metric and/or the coordinates of the vertices. The binomial distribution of the Hamming distances between the coordinates of a vertex and all the other vertices arises naturally from the angles of 2-face triangulation on $[n]$-cube (e.g., $\lambda \in \{0, 2, 2, 2, 4, 4, 4, 6\}$ for $n = 3$, cf. Fig 2).

The cotan Laplacian L of $[n]$-cube has the following additional properties to the cotan Laplacian (17) of any 2-dimensional triangulated surface (the list is not exhaustive; certain properties of L are possibly duplicated; (14) is assumed and binary or Gray encoding is necessary unless indicated otherwise):

- is bisymmetric, that is both symmetric ($L = L^T$) and centrosymmetric ($LJ = JL$, where J is the exchange matrix having 2^{n-1} eigenvalues +1 and 2^{n-1} eigenvalues −1);
- its eigengap (the difference between two successive eigenvalues) equals 2;
- its spectral radius equals $2n$;
- its trace equals $n2^n$;
- columns and rows of L are linearly dependent, so that Laplace's equation for $[n]$-cube, which is a homogeneous system
$$Lu = 0 \tag{19}$$
has a non-trivial solution;
- the solutions of (19) are constant vectors u_v (with all components equal) in any encoding; therefore if u_p is any specific solution to Poisson's equation for $[n]$-cube, which is the linear system
$$Lu = f \tag{20}$$
then the entire solution set can be described as $\{u_p + u_v\}$, where u_v is a constant vector solving Laplace's equation (19).

From Theorem 1 it follows that the discrete cotan Laplacian (17) is the same for any arrangement of 2-face diagonals including both diagonals on each 2-face. However, the adjacency matrices of such graphs depend on this arrangement. We found interesting properties of the spectrum of the adjacency matrix of $[n]$-cube if both diagonals are present.

Theorem 3. The maximum of the absolute values of all nontrivial eigenvalues of the adjacency matrix of the regular $[n]$-cube is

$$\lambda_2 := \max_{k \neq n} |\lambda_n| = \sum_{k=1}^{n} k - 2n = \frac{n(n-3)}{2} \tag{21}$$

(negation of A080956 OEIS sequence). Thus $\left(n + \binom{n}{2}\right)$-regular $[n]$-cube is Ramanujan graph for $n < 6$, that is

$$\frac{n(n-3)}{2} \leq 2\sqrt{n + \binom{n}{2} - 1} = 2\sqrt{\frac{n^2+n-2}{2}} \quad \Leftrightarrow \quad 1 < n < 6. \tag{22}$$

Proof. Direct calculation for consecutive n. The largest eigenvalue of the adjacency matrix of a d-regular graph, like an $[n]$-cube with both triangulations, is the vertex degree d. Hence, this is a trivial eigenvalue. A Ramanujan graph is a d-regular graph in which the second-largest eigenvalue in magnitude, which measures the graph's expansion properties, satisfies $\lambda_2 \leq 2\sqrt{d-1}$. □

Theorem 4. Integer values of the Ramanujan bound of regular $[n]$-cube (RHS of the inequality (22)) form A075848 OEIS sequence $\{0, 6, 36, 210, 1224, \dots\}$ are given by

$$\frac{3}{2\sqrt{2}}\left[(3+2\sqrt{2})^k - (3-2\sqrt{2})^k\right] \tag{23}$$

and n's yielding these integer values form A072221 OEIS sequence $\{1, 4, 25, 148, 865, \dots\}$ are given by

$$\frac{3}{4}\left[(3+2\sqrt{2})^k + (3-2\sqrt{2})^k\right] - \frac{1}{2}, \tag{24}$$

where $k \in \mathbb{N}_0$.

Proof. Direct calculation for consecutive n. □

In the case of n-cubes $\lambda_2 = n$ or $\lambda_2 = n - 2$ if we consider bipartite Ramanujan graphs, so the Ramanujan graph condition is satisfied only for $n = 2$ in the former case and for $4 - \sqrt{2} \leq n \leq 4 + \sqrt{2}$ (that is for $2 \leq n \leq 6$ if $n \in \mathbb{N}$) in the latter one. For $\{n\}$-cubes $\lambda_2 = -1$, so all $\{n\}$-cubes are Ramanujan graphs.

3 Fourth cube

The fourth cube contains 2^n of n-, $\{n\}$-, or $[n]$-cubes, wherein one vertex is common to all of them.

Definition 2. 2^n-cube is defined by 2^n n-cubes sharing common vertex address $\{0, 0, \dots, 0\}$.

This structure has 3^n vertices and

$$\binom{n}{k} 3^{n-k} 2^k \tag{25}$$

k-faces, $k = 0, 1, \dots, n$ (OEIS A038220) and the sum over k of all k-faces is 5^n. The number of addresses of 2^n-cube having the same Hamming weight is (OEIS A013609)

$$\binom{n}{k} 2^k. \tag{26}$$

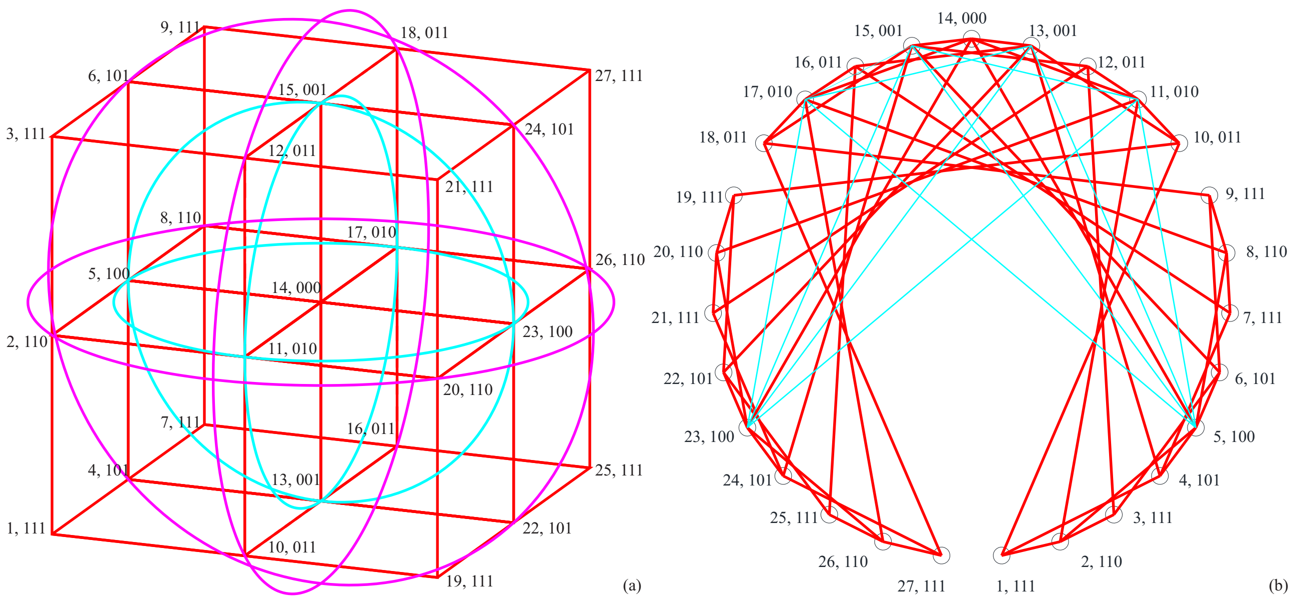

Figure 6: (a) unit and $\sqrt{2}$ radii (3)-balls in binary encoded 2^3-cube, (b) graph of this structure.

Definition 3. $[2^n]$-cube is 2^n-cube with triangulated 2-faces.

Definition 4. $\{2^n\}$-cube is defined by 2^n $\{n\}$-cubes sharing common vertex address $\{0, 0, \dots, 0\}$.

2^n-cube resembles the Cartesian coordinate system of $\mathbb{R}^n$, as shown in Fig. 6, wherein the signs of coordinates are provided by vertex indexation. In other words, 2^n-cube provides a bijective relation between the indices of 3^n vertices it comprises and their coordinates in n-dimensional space. 2^n-cube corresponds to unit n-cube, as shown in Fig. 7 for $n = 3$; there is only one central vertex 14 having address $a(14) = \{0, 0, 0\}$ from which one can recursively walk to six 1-norm vertices 13, 15; 11, 17 and 5, 23 by adding 3^k to or subtracting 3^k from the vertex index with $k = 0, 1, 2$ and modifying the corresponding bit of the new vertex address, and so on to 2-norm vertices up to 3-norm vertices 1, 3; 7, 9; 19, 21; 25, 27 having address $\{1, 1, 1\}$.

Nonetheless, the Hamming distance between vertices having different indices but the same addresses is zero, even though the Euclidean metric between the points having Cartesian coordinates induced by these vertices is between 2 and $2\sqrt{n}$. The Hamming distance between addresses of vertices 1 and 27 of 2^3-cube, for example, is 0, even though the Euclidean metric between Cartesian coordinates induced by these vertices is $2\sqrt{3}$.

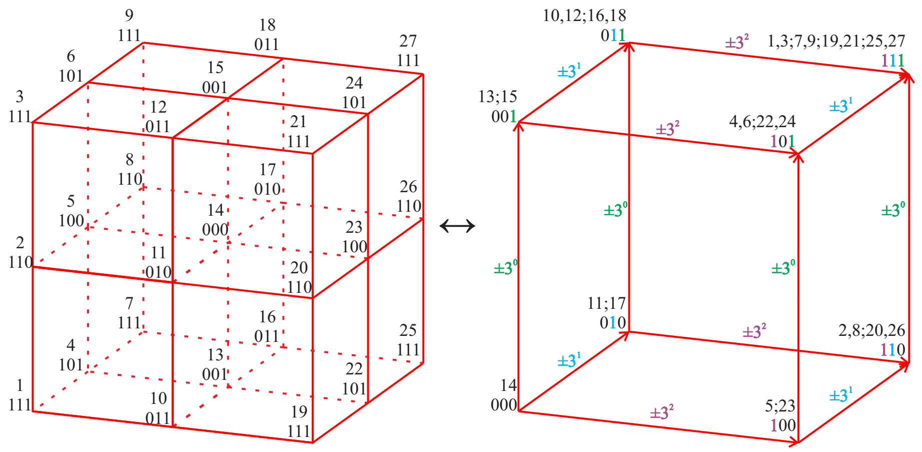

Figure 7: 2^n-cube index to address mapping (binary encoding) for $n = 3$.

Certain properties of these graphs are discussed below.

Theorem 5. The spectrum of the adjacency matrix of 2^n-cube in Gray or binary encoding is symmetric, degenerate (for $n \geq 2$), and includes all multiplicities of $\sqrt{2}$ from $-n\sqrt{2}$ to $n\sqrt{2}$. Multiplicities of the same eigenvalues form a trinomial triangle.

Proof. Direct calculation for consecutive n. □

Theorem 6. The spectrum of the cotan Laplacian (17) of $[2^n]$-cube in Gray or binary encoding is degenerate and includes all integers from 0 to $3n$ without the eigenvalue of $3n - 1$. Multiplicities of the same eigenvalues form A038717 OEIS sequence.

Proof. Direct calculation for consecutive n. □

Some of the further properties of the cotan Laplacian of the $[2^n]$-cube are (again assuming positive weights (14) and binary or Gray ordering of vertices to center the origin):

- it is bisymmetric;
- its diagonal entries span from n to $2n$;
- its spectral gap (the difference between the two largest eigenvalues) equals 2; otherwise, the eigengap is 1;
- its spectral radius equals $3n$;
- it has $\lceil 3^n/2 \rceil$ symmetric ($Jx_S = x_S$) orthonormal eigenvectors x_S and $\lfloor 3^n/2 \rfloor$ antisymmetric ($Jx_A = -x_A$) orthonormal eigenvectors x_A [31];

2^n-cube enables to inscribe all n-balls having radii $\sqrt{k}$, where $k \in \{1, 2, \ldots, n\}$ inside it (Disc in 4 squares, ball in 8 cubes, etc.), having surfaces kissing all vertices having addresses distanced k bits from the center, as shown in Fig. 6 and 8 .

Theorem 7. The distance matrix for binary and Gray encoded 2^n-cube is the same.

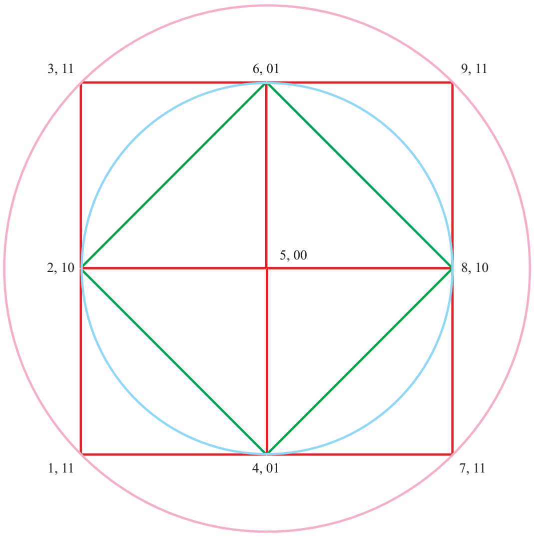

Figure 8: Unit and $\sqrt{2}$ radii (2)-balls in binary encoded $[2^2]$-cube.

Proof. Direct calculation for consecutive n. Both binary and Gray encoding give the same norms of the addresses with the index $m = \lfloor 3^n/2 \rfloor + 1$ as the origin. □

Theorem 8. The spectrum of the bisymmetric distance matrix of 2^n-cube has a distinct irrational minimum negative eigenvalue and a distinct irrational maximum positive eigenvalue given by

$$\lambda_{\min/\max}(n) = \left[2(n-1) \mp \sqrt{2(2n+1)(n+2)}\right] 3^{n-2}, \tag{27}$$

and contains $n-1$ integer negative eigenvalues given by

$$\lambda_2 = -4 \cdot 3^{n-2} \tag{28}$$

and $3^n - n - 1$ (OEIS A060188) zero eigenvalues.

Proof. Direct calculation for consecutive n. □

The sums $\{0, 4, 24, 108, \ldots\}$ of the eigenvalues (27) satisfy

$$\lambda_{\min} + \lambda_{\max} = 4(n-1)3^{n-2} \tag{29}$$

which is the OEIS integer sequence A120908, while the products $-\{2, 36, 486, 5832, \ldots\}$ of the eigenvalues (27) satisfy

$$\lambda_{\min}\lambda_{\max} = -2n3^{2n-2} \tag{30}$$

forming the integer sequence, which is close to the OEIS sequence A288834 (every 2nd entry's modulus agrees). Also $|\lambda_{\min}(7) + \lambda_{\max}(7)| = |-\lambda_{\min}(4)\lambda_{\max}(4)| = 5832$ is the only common value in modulus shared by the sums (29) and products (30). The eigenvalues (28) form the opposite of the OEIS sequence A003946 for $n \geq 2$ and the sum of all eigenvalues of the distance matrix of 2^n-cube vanishes.

An n-dimensional simplicial companion of 2^n-cube is n-vector equilibrium, a structure featuring radial equilateral symmetry (circumradius equals the edge length) for any $n \in \mathbb{N}$ defined by Buckminster Fuller for $n = 3$. External vertices of n-vector equilibria are vertices of Stott expanded regular simplices by their dual ones, polytopes forming a dimensional sequence listed [32] in Table 2. All these polytopes (for $n \geq 1$) are 3-layered stacks of vertex layers. The convex hull of the 1st layer is the corresponding $(n-1)$-simplex, which thus is a true facet of that polytope, the convex hull (cross-section) of the 2nd, equatorial layer is that expanded $(n-1)$-simplex, and the convex hull of the 3rd layer is the $(n-1)$-simplex, dual to the $(n-1)$-simplex of the 1st layer. A comparison of 2^n-cubes and n-vector equilibrium is illustrated in Table 1 for $n \leq 3$. The number of the external (other than the origin) vertices $|v(n)|$ of the n-vector equilibrium is A279019 OEIS sequence, the least possible number

Table 1: 2^n-cubes and n-vector equilibria.

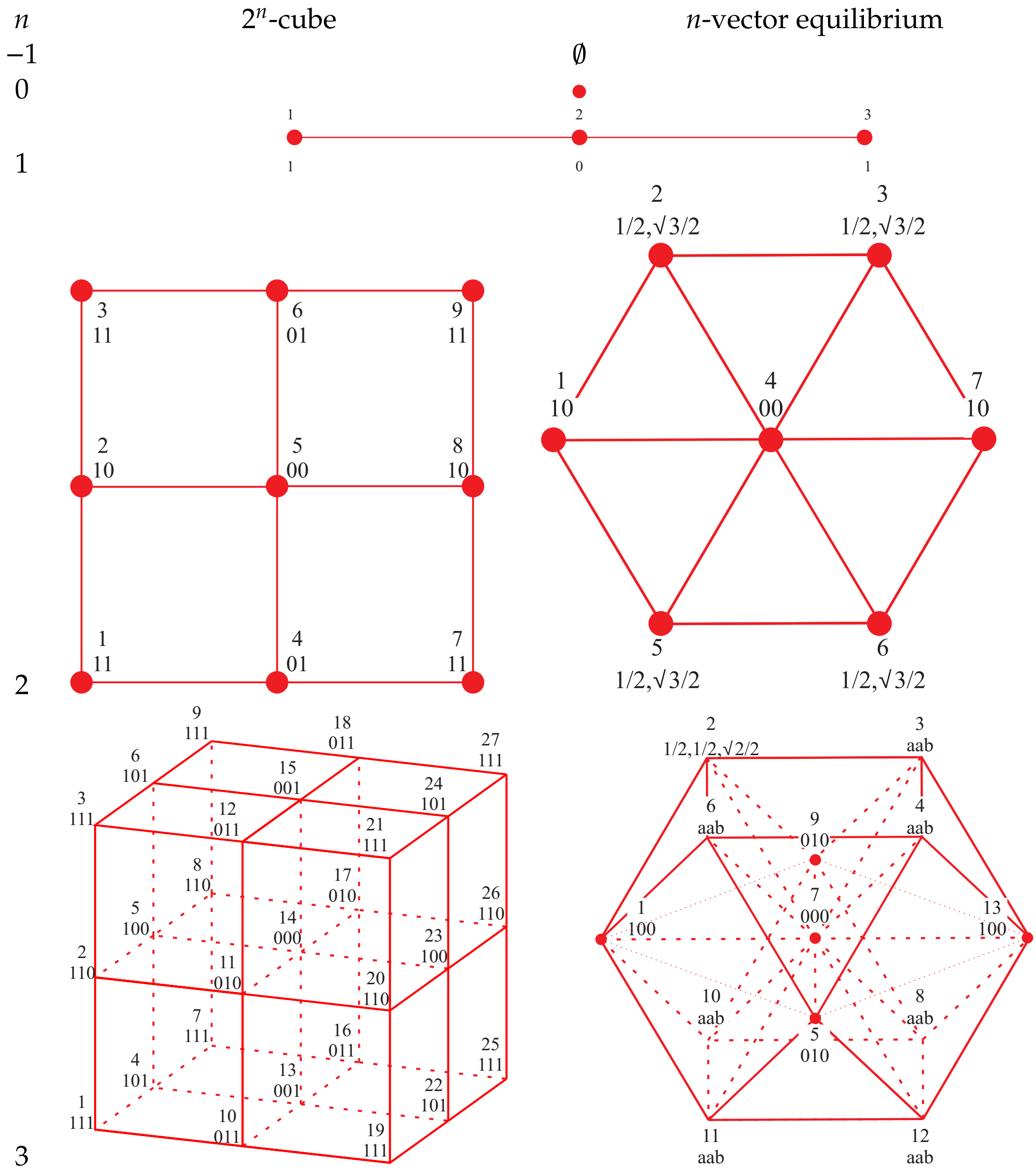

Table 2: Stott expanded regular simplices by their dual ones.

n	Dynkin diagram	name	$\lvert v(n)\rvert$
−1	∅	empty set	0
0	1	point	0
1	3	two line segments	2
2	x3x=6	regular hexagon	6
3	x3o3x=co	cuboctahedron	12
4	x3o3o3x=spid	runcinated 4-simplex	20
5	x3o3o3o3x=scad	stericated 5-simplex	30
6	x3o3o3o3o3x=staf	pentellated 6-simplex	42
7	x3o3o3o3o3o3x=suph	hexicated 7-simplex	56
8	x3o3o3o3o3o3o3x=soxeb	heptellated 8-simplex	72

of diagonals of a simple convex polyhedron with n faces, which is also twice the sum of the natural numbers less than or equal n, and can also be obtained by the following recurrence

$$|v(n)| = n(n+1) = 2\sum_{k=0}^{n} k = |v(n-1)| + 2n, \quad |v(-1)| := 0. \tag{31}$$

$|v(n)|$ equals the kissing number of $\mathbb{R}^n$, the greatest number of non-overlapping unit spheres that can be arranged in $\mathbb{R}^n$ such that they each touch a common unit sphere, for $1 \leq n \leq 3$. But $|v(n)|$ (31) grows much slower than the kissing number for $n \geq 4$. For $2 \leq n \leq 3$, an n-vector equilibrium can be oriented in $\mathbb{R}^n$ such that its $2(n-1)$ external vertices and the central vertex define a Cartesian coordinate system for $\mathbb{R}^{n-1}$. This cannot be done for $n > 3$ as the number of the remaining external vertices is $|v(n)| - 2(n-1) = n^2 - n + 2$, while 2^n is required, and $n^2 - n + 2 = 2^n$ only for $1 \leq n \leq 3$.

Cubes follow generalized principles (that is, the rules that hold without exception, according to Buckminster Fuller [33] (p. 16)) with regard to their dimensionality (allowing for direct calculation for consecutive n), although they do not provide optimal energetic conditions. Unit 3-balls, for example, placed in the vertices of 2^3-cube will not form a spatially optimal and stable arrangement. Conversely, n-vector equilibria do not follow generalized principles but seem to follow synergetic principles, guiding the works of nature [33] (p. 5).

4 Discussion

Biological evolution is a change in the heritable characteristics of biological populations of individuals over their successive generations. These characteristics are the information passed on from an individual parent(s) to the individual offspring during reproduction. Evolution is the process by which traits that enhance survival and reproduction become more common in successive population generations, wherein

1. variation of phenotypic traits exists within populations of individuals;
2. different traits confer different rates of survival and reproduction; and
3. these traits can be passed from generation to generation.

An individual is a perceiving entity. A cell, an organism, a biological neural network, a liquid brain [34] in particular. But not a virus, DNA, or AI. Perception is a mapping between external information (the individual's *Umwelt*) and corresponding memorized information stored in the individual's memory. Hence, information exists only due to this mapping, and the SDM is ideal for storing a predictive model of the world [14]. It has been demonstrated [35] that the process of memorizing information does not require neural networks. Memory has evolved solely to enable reproductive fitness. It is a memory that enables one to perceive movement despite Zeno's paradoxes of motion.

Only for $\mathbb{R}^4$ there exists an uncountable family of non-diffeomorphic differentiable structures which are homeomorphic to $\mathbb{R}^4$ [36] (for every such smooth structure, there exists a simplicial triangulation, its discrete version [37]. This property is known as exotic $\mathbb{R}^4$. For $n \in \{1, 2, 3\}$, any smooth manifold homeomorphic to $\mathbb{R}^n$ is also diffeomorphic to $\mathbb{R}^n$. For $n > 4$, examples of homeomorphic but not diffeomorphic pairs on spheres have been found but are countable (cf. Milnor's sphere for $n = 7$). For $n \neq 4$ exotic $\mathbb{R}^n$'s do not exist [38].

This feature of 4-dimensional space that we perceive indicates that it is necessary for biological evolution. Indeed, for $n \in \{1, 2, 3\}$, any differentiable structure perceived by an individual would be diffeomorphic to the corresponding differentiable structure that this individual has already memorized. There would be only one equivalence class between them. This, in turn, would contradict the principles of biological evolution: no variations of traits would exist, the same traits would confer the same rates of survival and reproduction, and there would be no need to pass these same traits from generation to generation. That implies that only $n = 3 + 0i$ dimensions allow for variations of traits between any two individuals that perceive the same differentiable structure. Dimension $n > 4$ provides examples of homeomorphic but not diffeomorphic pairs of differentiable structures. But their number is finite, so a sufficiently large population of individuals would soon saturate this set, and the evolution would terminate. Physical objects are not the objective reality; they are simply elements of one's user interface [39]. But because of the exotic $\mathbb{R}^4$, these elements must be perceived instantaneously as 3-dimensional.

We acknowledge that the claimed necessity of four-dimensional perception was not rigorously demonstrated in this study, as we did not address the mechanism by which a biological organism's perception of a differentiable structure (a mathematical abstraction) is mapped into a memorized predictive model. A rigorous demonstration of this claim may be difficult due to the fundamentally incomputable nature of living organisms [40].

Observer independence has been invalidated in a quantum photonic experiment [41] (implementing the gedanken experiment proposed in [42], which demonstrated that no general framework exists in which all observers can reconcile all their recorded facts. That means there is no (single or unique) objective reality that an observer could perceive and communicate to another. This by no means boils down to subjectivism since the existence of observer-dependent (aka subjective) facts, as such, does not preclude the existence of an observer-independent, general framework. But such a framework would contradict the results of this experiment.

Also, the UDT asserts that an observer-independent (objective) reality cannot be constructed by observer-independent facts, i.e., equally similar (i.e., the same) objects, particles, etc. The UDT holds trivially for points in a space: any two points are equally similar insofar as they are distinguishable. The corollary of the UDT (assigning individual weights to the predicates (6) to assert the similarity of the objects) is just the 2nd fact of evolution (differential fitness). Some individuals do it locally better, some do it locally worse. One simply *learns to discern* and for $n = 4$ every individual memorizes its own unique version of observer-dependent reality that it perceives through the $(2 + 0i)$-dimensional holographic sphere of perception, triangulated with Planck areas corresponding to bits of information.

Acknowledgments

As always, I truly thank my wife for her support during the turbulent 2020 pandemic, when this research was conducted. I also thank Rafał Winiarski for his feedback concerning Watanabe's implicational constraints, and Wawrzyniec Bieniawski, Piotr Masierak, and Andrzej Tomski for numerous clarity and formal corrections, and improvements.

References

[1] M. H. Poincaré. Sur la dynamique de l'électron. Rendiconti del Circolo matematico di Palermo, 21(1):129–175, December 1906.

[2] Karl Friston, James Kilner, and Lee Harrison. A free energy principle for the brain. Journal of Physiology-Paris, 100(1–3):70–87, July 2006.

[3] Karl Friston. A free energy principle for a particular physics, 2019.

[4] Ludwig Boltzmann. Über die Beziehung zwischen dem zweiten Hauptsatze der mechanischen Wärmetheorie und der Wahrscheinlichkeitsrechnung resp. den Sätzen über das Wärmegleichgewicht. Cambridge Library Collection - Physical Sciences, volume 2, pages 164–223. Cambridge University Press, 2012.

[5] Thomas S. Kuhn. Black-body theory and the quantum discontinuity: 1894–1912. Clarendon Press, Oxford, 1978.

[6] A. N. Kolmogorov. Combinatorial foundations of information theory and the calculus of probabilities. Russian Mathematical Surveys, 38(4):29–40, August 1983.

[7] Mioara Mugur-Schachter. On a Crucial Problem in Probabilities and Solution, 2008.

[8] David Jennings and Matthew Leifer. No return to classical reality. Contemporary Physics, 57(1):60–82, January 2016.

[9] Michael Levin. Self-Improvising Memory: A Perspective on Memories as Agential, Dynamically Reinterpreting Cognitive Glue. Entropy, 26(6):481, May 2024.

[10] Mathieu Desbrun, Eva Kanso, and Yiying Tong. Discrete differential forms for computational modeling. In ACM SIGGRAPH ASIA 2008 courses on - SIGGRAPH Asia '08, pages 1–17, Singapore, 2008. ACM Press.

[11] Anil Nirmal Hirani. Discrete exterior calculus. PhD thesis, California Institute of Technology, June 2003.

[12] Szymon Łukaszyk and Andrzej Tomski. Omnidimensional Convex Polytopes. Symmetry, 15(3):755, March 2023.

[13] Andrei Markov. Regular Polytopes in $\mathbb{Z}^n$, 2011.

[14] Pentti Kanerva. Sparse distributed memory. MIT Press, Cambridge, Mass, 1988.

[15] Satosi Watanabe. Epistemological Relativity. Annals of the Japan Association for Philosophy of Science, 7(1):1–14, 1986.

[16] S. Lukaszyk. A new concept of probability metric and its applications in approximation of scattered data sets. Computational Mechanics, 33(4):299–304, March 2004.

[17] Satoshi Watanabe. Knowing and guessing: a quantitative study of inference and information. Wiley, New York, 1969.

[18] Tomasz Szandała. Review and Comparison of Commonly Used Activation Functions for Deep Neural Networks. In Akash Kumar Bhoi et al., editors, Bio-inspired Neurocomputing, volume 903, pages 203–224. Springer Singapore, 2021.

[19] Andrea Apicella, Francesco Donnarumma, Francesco Isgrò, and Roberto Prevete. A survey on modern trainable activation functions. Neural Networks, 138:14–32, June 2021.

[20] Krishnagopal Dharani. Dendrites and Primary Thoughts. In The Biology of Thought, pages 109–122. Elsevier, 2015.

[21] Ilya Prigogine and Isabelle Stengers. Order out of Chaos: Man's New Dialogue with Nature. Bantam Books, 1984.

[22] Chris Fields, James F. Glazebrook, and Antonino Marcianò. Reference Frame Induced Symmetry Breaking on Holographic Screens. Symmetry, 13(3):408, March 2021.

[23] Szymon Łukaszyk. Black Hole Horizons as Patternless Binary Messages and Markers of Dimensionality, chapter 15, pages 317–374. Nova Science Publishers, 2023.

[24] G. 't Hooft. Dimensional Reduction in Quantum Gravity, 1993.

[25] Szymon Łukaszyk. Life as the explanation of the measurement problem. Journal of Physics: Conference Series, 2701(1):012124, February 2024.

[26] Keenan Crane. The n-dimensional cotangent formula. `https://www.cs.cmu.edu/~kmcrane/Projects/Other/nDCotanFormula.pdf`, 2019. Accessed: 2025-07-13.

[27] Max Wardetzky. A Primer on Laplacians. Taylor & Francis, CRC Press, Boca Raton, 2017.

[28] Renjie Chen, Yin Xu, Craig Gotsman, and Ligang Liu. A spectral characterization of the Delaunay triangulation. Computer Aided Geometric Design, 27(4):295–300, May 2010.

[29] Samuel Rippa. Minimal roughness property of the Delaunay triangulation. Computer Aided Geometric Design, 7(6):489–497, November 1990.

[30] Charles L. Lawson. Transforming triangulations. Discrete Mathematics, 3(4):365–372, 1972.

[31] A. Cantoni and P. Butler. Eigenvalues and eigenvectors of symmetric centrosymmetric matrices. Linear Algebra and its Applications, 13(3):275–288, 1976.

[32] Klitzing. Re: what is the 5d vector equilibrium? `http://hi.gher.space/forum/viewtopic.php?f=32&t=2207#p25149`, 2016. Accessed: 2025-07-13.

[33] Amy C. Edmondson. A Fuller Explanation. Birkhäuser Boston, Boston, MA, 1987.

[34] Ricard Solé, Melanie Moses, and Stephanie Forrest. Liquid brains, solid brains. Philosophical Transactions of the Royal Society B: Biological Sciences, 374(1774):20190040, June 2019.

[35] Monica Gagliano, Michael Renton, Martial Depczynski, and Stefano Mancuso. Experience teaches plants to learn faster and forget slower in environments where it matters. Oecologia, 175(1):63–72, May 2014.

[36] Clifford Henry Taubes. Gauge theory on asymptotically periodic 4-manifolds. Journal of Differential Geometry, 25(3), January 1987.

[37] Robion C. Kirby and L. Siebenmann. Foundational essays on topological manifolds, smoothings, and triangulations. Annals of mathematics studies, no. 88. Princeton University Press, Princeton, N.J, 1977.

[38] Robert E. Gompf. Three exotic R4's and other anomalies. Journal of Differential Geometry, 18(2), January 1983.

[39] Donald D. Hoffman. Sensory Experiences as Cryptic Symbols of a Multimodal User Interface. Activitas Nervosa Superior, 52(3–4):95–104, September 2010.

[40] Johannes Jaeger, Anna Riedl, Alex Djedovic, John Vervaeke, and Denis Walsh. Naturalizing relevance realization: why agency and cognition are fundamentally not computational. Frontiers in Psychology, 15:1362658, June 2024.

[41] Massimiliano Proietti, Alexander Pickston, Francesco Graffitti, Peter Barrow, Dmytro Kundys, Cyril Branciard, Martin Ringbauer, and Alessandro Fedrizzi. Experimental test of local observer independence. Science Advances, 5(9):eaaw9832, September 2019.

[42] Časlav Brukner. On the Quantum Measurement Problem. In Reinhold Bertlmann and Anton Zeilinger, editors, Quantum [Un]Speakables II, pages 95–117. Springer International Publishing, Cham, 2017.